Research Square

Preprints are preliminary reports that have not undergone peer review.
They should not be considered conclusive, used to inform clinical practice,
or referenced by the media as validated information.

ZnO and CuO nanoparticles prepared via the co-precipitation method: the evaluation of morphology and formation mechanism

Narges Johari (johari_narges@yahoo.com)
Golpayegan University of Technology
Faezeh Zohari
Golpayegan University of Technology
Fatemeh Rafati
Golpayegan University of Technology

Research Article

Keywords: ZnO nanoparticles, CuO nanoparticles, Co-precipitation method, Flower-like structure, Sphere-like structure, nanoprism structure

Posted Date: June 22nd, 2021

DOI: https://doi.org/10.21203/rs.3.rs-640074/v1

License: This work is licensed under a Creative Commons Attribution 4.0 International License.
Read Full License

Abstract

The morphology of nanomaterials is an important factor to determine their properties. In this study, zinc oxide (ZnO) and cupric oxide (CuO) nanoparticles were synthesized via the co-precipitation method with the same protocols. Zinc nitrate and copper sulfate were selected as ZnO and CuO precursors, respectively. Then, the phase structure and morphology of both prepared nanoparticles were investigated and showed that ZnO and CuO were prepared without any impurities and with different morphologies. The obtained ZnO and CuO nanoparticles illustrated sphere-like and hierarchical flower-like structures, respectively, due to their various phase structure and electrostatic interactions.

1. Introduction

Recently, nanomaterials have been significantly considered due to their large area to volume ratio, leading to their special electrical, chemical, mechanical, physical, optical, and magnetical properties [1]. Among the nano-sized materials, zinc oxide (ZnO) nanoparticles is an important metal oxide with specific physical and chemical properties utilized in different fields [2, 3], such as the rubber composite's wear-proof, polymer antiaging, polymer toughening [4], strong UV absorber in cosmetics and sunscreen [5], fiber additive in the textile industry for UV and visible light resistance [6], photo-catalyst [7], concrete productive [8], etc. In addition, zinc is an essential trace element in bone, skin, muscle, brain, and various enzyme systems [9, 10], which then causes the use of ZnO nanoparticles as the food and drug additive [11].

Further, cupric oxide (CuO) is a p-type semiconductor metal oxide with narrow band gap [12] employed in electronic device [13], electrochemical cells [14], sensors [15], solar cells [16], catalysts [17], and so on. Furthermore, copper and its complexes are utilized as antimicrobial agents in water purification, textile, and biomedical devices [18–20].

The morphology of nanostructures is an important factor to determine the properties of materials [1]. Various morphologies, such as nano-rods [21], nano-sphere [22], nano-flakes [23], nano-whiskers [24], etc. have been studied in nanomaterials and revealed different properties. Several parameters, such as preparation technique [25], temperature [26], pressure [27], and precursor concentrations [28] possess the most important role to form different morphologies for nanomaterials.

In the current study, Cuo and ZnO nanoparticles were synthesized via the co-precipitation method. In the synthesis stages of both nanoparticles were used the same protocols. The only difference in the protocols of the preparation of ZnO and CuO nanoparticles was in the selection of their salt precursors. ZnO and CuO salt precursors were selected zinc nitrate and copper sulfate, respectively. Then, the ultimate morphology of both obtained nanoparticles was investigated.

2. Materials And Methods

2.1. Synthesis of ZnO nanoparticles

ZnO nanoparticles were synthesized via the co-precipitation method. Accordingly, two different solutions were prepared, named solution A and solution B. To prepare solution A, zinc nitrate ($Zn(NO_3)_2$, Sigma-Aldrich) was added into deionized water with 0.5 Molar of concentration and stirred at 60 °C. Solution B was a 2 Molar solution of sodium hydroxide (NaOH, Merck). Then, solution B was slowly dripped with the rate of 15 drops/min into solution A which stirred at 60 °C. During the dripping, the pH of the obtained solution was measured frequently. with the increase of the pH of the solution, white precipitations were formed, suspended, and increased gradually. When the pH of the obtained suspension reached around 14, the dripping of solution B was stopped, then the suspension was frequently rinsed by using of distilled water until the ultimate suspension pH measured equal to 7. Finally, the obtained white precipitations were filtered and dried in an oven at 100 °C for 12 hr.

2.2. synthesis of CuO nanoparticles

To synthesis CuO nanoparticles using the co-precipitation method, two solutions named C and D were prepared. Solution C and D were a 0.5 Molar solution of copper sulfate ($CuSO_4$, Merck), and a 2 Molar solution of NaOH. To obtain CuO nanoparticles, solution D was added into solution C exactly similar to the protocol used for synthesizing ZnO nanoparticles described in Sect. 2.1. The color of dried obtained CuO nanoparticles was dark brown or black.

2.3. Phase structure study

The crystallinity and phase structure of the synthesized ZnO and CuO nanoparticles were investigated using X-ray diffractometer (XRD, PAN analytical, The Netherlands), measured via CuKα radiations at the wavelength of 1.54 Å in the angular range of 10–90 °.

2.4. Morphological study

The morphology of synthesized ZnO and CuO nanoparticles was evaluated via field emission scanning electron microscopy (FESEM, TESCAN, Czech Republic) and attached with energy dispersive spectroscopy (EDS) for elemental analysis.

3. Results And Discussions

XRD pattern of the synthesized CuO nanoparticles is shown in Fig. 1A which is indexed to the monoclinic CuO phase with relatively broad peaks conformed with lattice constants of JCPDS card No. 96-101-1195. In addition, the broadening of the XRD peaks is suggesting the presence of the nano-sized crystals and, no impurity peak was observed in obtained XRD pattern. Also, as shown in Fig. 1B, EDS analysis of synthesized nanoparticles reveals the presence of Cu to O.

Figure 2 exhibits FESEM images of the prepared CuO nanoparticles with a hierarchical structure composed of nanoflakes which created the flower-like CuO particles. The thickness of nanoflakes was

measured around 65 ± 26 nm via Image J software. Also, the diameter of CuO flower-like particles was measured about 500 ± 112 nm.

According to FESEM images, first, CuO nanoflakes were formed then interlocked with each other to create CuO flower-like particles. According to Yu et al. [29] suggestion, the formation of CuO flower-like particles has occurred in several stages mentioned follow as: (1) the growth of some shuttle-shaped CuO nanoflakes, (2) the emerging and growth of more nanoflakes with smaller size, and (3) the newly CuO precipitation radiated orientation from the previous center. Accordingly, the reactions that result in the nucleation and growth of CuO flower-like particles as follows: (1) dissolution of Cu in the form of [Cu(OH)4]2− indicated in Eq. 1, (2) Nucleation of CuO as is shown in Eq. 2, (3) the growth of CuO nanoflaks on CuO grains, and (4) the growth of larger CuO grains and dissolution of smaller ones.

$$Cu2 + + 4OH- \rightarrow [Cu(OH)4]2- \quad (1)$$

$$Cu(OH)42- \rightarrow CuO + H2O + 2OH- \quad (2)$$

Besides, as shown in Fig. 1A, the strongest reflections belong to (111) and (111-) planes which indicated the first oriented growth planes of CuO. Indeed, [Cu(OH)4]2− ions were oriented and grown along (111) and (111-) planes [30, 31]. [Cu(OH)4]2− anion group is an inorganic precursor to form CuO particles [32]. Indeed, two OH− groups bound to two Cu2 + cations formed an H2O molecule and two Cu2 + cations are bridged via O2, resulting in forming chains of square planar CuO4 groups, then CuO precipitations. The formation tendency of [Cu(OH)4]2− anion group is in spherical clusters, resulting in the nucleation of CuO nanoflakes after condensation [33, 34]. By reducing the concentration of [Cu(OH)4]2− the packing probability of CuO decreases, leading to slow nucleation of CuO with layered and flak-shape structures. While by increasing the concentration of OH−, CuO tends to agglomerate without layered structure [33, 35]. Due to Ostwald ripening and the disparity in surface-to-volume ratio, the small nanoflakes and crystals disappear and further enlargement ones leave and grow, then develop to flower-like structure [29, 36].

On the other hand, Fig. 3A shows the XRD pattern of the synthesized ZnO nanoparticles with hexagonal phase structure that matched with lattice constants of JCPDS card No. 96-901-1663. The DSC analysis of prepared ZnO nanoparticles shows in Fig. 3B revealed the presence of Zn and O in the spot detection. Further, Fig. 3C illustrated the comparison of XRD patterns and phase structure of both synthesized ZnO and CuO revealed that the obtained peaks of CuO are broader than of ZnO. Namely, the structure of the synthesized CuO particles is finer than ZnO. To confirm this result, the average particle size of prepared nanoparticles was measured around 88 ± 35 using Image J software.

Figure 4A illustrates the morphology of the prepared ZnO nanoparticles by using FESEM images displayed sphere-like structure with a few prism-like nanoparticles (as shown in Fig. 4B). To form the sphere-like ZnO nanoparticles, the electrostatic interactions between $[Zn(OH)4]^{2-}$ and polar surfaces possess the main role in ZnO nucleation. In presence of NaOH, $[Zn(OH)4]^{2-}$ anions obtained from the following equation:

$Zn2++4OH- \rightarrow [Zn(OH)4]2-$ (3)

According to Wen et al. [37] study, NaOH concentration specifies that either $[Zn(OH)4]2-$ growth units are enough to grow ZnO. Here, 2 Molar NaOH solution provided a weak electrostatic interaction between $[Zn(OH)4]^{2-}$ and polar surfaces, then both sphere-like ZnO nanoparticles and nano-ZnO with preferred orientation in a nano-prism structure formed [37, 38].

Indeed, as a suggestion, the difference between the crystal structures of ZnO and CuO nanoparticles and various electrostatic interactions between their anions and polar surfaces leads to their different structures.

4. Conclusion

In the present study, ZnO and CuO nanoparticles were synthesized using the co-precipitation method with the same protocols. The phase structure and morphology of the prepared nanoparticles were evaluated and revealed that the nanoparticles were synthesized without any impurities, while they had different morphologies. ZnO nanoparticles possessed sphere-like structure with a few nano-prism, although CuO nanoparticles exhibited hierarchical flower-like structure created from nano-flakes. In summary, the difference between the crystal structures of ZnO and CuO nanoparticles and various electrostatic interactions between their anions and polar surfaces leads to their different structures.

Declarations

Conflict of interest

The authors declare that they have no conflict of interest.

References

1. V.V. Gopal, S. Kamila, Effect of temperature on the morphology of ZnO nanoparticles: a comparative study, Applied Nanoscience 7(3–4) (2017) 75–82.
2. R.E. Adam, G. Pozina, M. Willander, O. Nur, Synthesis of ZnO nanoparticles by co-precipitation method for solar driven photodegradation of Congo red dye at different pH, Photonics Nanostructures-Fundamentals Applications 32 (2018) 11–18.
3. J. Jiang, J. Pi, J. Cai, The advancing of zinc oxide nanoparticles for biomedical applications, Bioinorganic chemistry applications 2018 (2018).
4. A. Kołodziejczak-Radzimska, T. Jesionowski, Zinc oxide—from synthesis to application: a review, Materials 7(4) (2014) 2833–2881.
5. S. Nayak, A. Chaudhari, B. Vaidhun, Synthesis, characterization and ameliorative properties of food, formulation and cosmetic additives: Case study of Zinc oxide nanoparticles, Journal of Excipients Food Chemicals 11(4) (2020) 79–92.

6. A.K. Anbalagan, S. Gupta, A. Kumar, S.-C. Haw, S.S. Kulkarni, N.-H. Tai, F.-G. Tseng, K.C. Hwang, C.-H. Lee, Gamma Ray Irradiation Enhances the Linkage of Cotton Fabrics Coated with ZnO Nanoparticles, ACS omega 5(25) (2020) 15129–15135.
7. M. Golmohammadi, M. Honarmand, S. Ghanbari, A green approach to synthesis of ZnO nanoparticles using jujube fruit extract and their application in photocatalytic degradation of organic dyes, Spectrochimica Acta Part A: Molecular Biomolecular Spectroscopy 229 (2020) 117961.
8. M. Kumar, M. Bansal, R. Garg, An overview of beneficiary aspects of zinc oxide nanoparticles on performance of cement composites, Materials Today: Proceedings 43 (2021) 892–898.
9. R. Alimohamady, H. Aliarabi, R.M. Bruckmaier, R.G. Christensen, Effect of different sources of supplemental zinc on performance, nutrient digestibility, and antioxidant enzyme activities in lambs, Biological trace element research 189(1) (2019) 75–84.
10. S. Huang, W. Wu, Y. Su, L. Qiao, Y. Yan, Insight into the corrosion behaviour and degradation mechanism of pure zinc in simulated body fluid, Corrosion Science 178 (2021) 109071.
11. J. Machotová, A. Kalendová, M. Voleská, D. Steinerová, M. Pejchalová, P. Knotek, L. Zárybnická, Waterborne hygienic coatings based on self-crosslinking acrylic latex with embedded inorganic nanoparticles: a comparison of nanostructured ZnO and MgO as antibacterial additives, Progress in Organic Coatings 147 (2020) 105704.
12. A. El-Trass, H. ElShamy, I. El-Mehasseb, M. El-Kemary, CuO nanoparticles: synthesis, characterization, optical properties and interaction with amino acids, Applied Surface Science 258(7) (2012) 2997–3001.
13. J. Sultana, S. Paul, R. Saha, S. Sikdar, A. Karmakar, S. Chattopadhyay, Optical and electronic properties of chemical bath deposited p-CuO and n-ZnO nanowires on silicon substrates: p-CuO/n-ZnO nanowires solar cells with high open-circuit voltage and short-circuit current, Thin Solid Films 699 (2020) 137861.
14. R. Ahmad, M. Khan, P. Mishra, N. Jahan, M.A. Ahsan, I. Ahmad, M.R. Khan, Y. Watanabe, M.A. Syed, H. Furukawa, Engineered hierarchical CuO nanoleaves based electrochemical nonenzymatic biosensor for glucose detection, Journal of the Electrochemical Society 168(1) (2021) 017501.
15. P. Patil, U.T. Nakate, Y.T. Nakate, R.C. Ambare, Acetaldehyde sensing properties using ultrafine CuO nanoparticles, Materials Science in Semiconductor Processing 101 (2019) 76–81.
16. R. Tan, Z. Wei, J. Liang, Z. Lv, B. Chen, J. Qu, W. Yan, J. Ma, Enhanced open-circuit photovoltage and charge collection realized in pearl-like NiO/CuO composite nanowires based p-type dye sensitized solar cells, Materials Research Bulletin 116 (2019) 131–136.
17. Y. Pan, S. Jiang, W. Xiong, D. Liu, M. Li, B. He, X. Fan, D. Luo, Supported CuO catalysts on metal-organic framework (Cu-UiO-66) for efficient catalytic wet peroxide oxidation of 4-chlorophenol in wastewater, Microporous and Mesoporous Materials 291 (2020) 109703.
18. H. Almasi, P. Jafarzadeh, L. Mehryar, Fabrication of novel nanohybrids by impregnation of CuO nanoparticles into bacterial cellulose and chitosan nanofibers: Characterization, antimicrobial and release properties, Carbohydrate polymers 186 (2018) 273–281.

19. T.I. Shaheen, A. Fouda, S.S. Salem, Integration of cotton fabrics with biosynthesized CuO nanoparticles for bactericidal activity in the terms of their cytotoxicity assessment, Industrial Engineering Chemistry Research 60(4) (2021) 1553–1563.
20. S. Tharchanaa, K. Priyanka, K. Preethi, G. Shanmugavelayutham, Facile synthesis of Cu and CuO nanoparticles from copper scrap using plasma arc discharge method and evaluation of antibacterial activity, Materials Technology 36(2) (2021) 97–104.
21. R. Baiyasi, M.J. Gallagher, L.A. McCarthy, E.K. Searles, Q. Zhang, S. Link, C.F. Landes, Quantitative Analysis of Nanorod Aggregation and Morphology from Scanning Electron Micrographs Using SEMseg, The Journal of Physical Chemistry A 124(25) (2020) 5262–5270.
22. Y. Fatieiev, J.G. Croissant, K. Alamoudi, N.M. Khashab, Cellular internalization and biocompatibility of periodic mesoporous organosilica nanoparticles with tunable morphologies: from nanospheres to nanowires, ChemPlusChem 82(4) (2017) 631–637.
23. X. Wang, J. He, B. Yu, B. Sun, D. Yang, X. Zhang, Q. Zhang, W. Zhang, L. Gu, Y. Chen, CoSe2 nanoparticles embedded MOF-derived Co-NC nanoflake arrays as efficient and stable electrocatalyst for hydrogen evolution reaction, Applied Catalysis B: Environmental 258 (2019) 117996.
24. S. Habibi, M. Jamshidi, Synthesis of TiO2 nanoparticles coated on cellulose nanofibers with different morphologies: Effect of the template and sol-gel parameters, Materials Science in Semiconductor Processing 109 (2020) 104927.
25. D. Dastan, Effect of preparation methods on the properties of titania nanoparticles: solvothermal versus sol–gel, Applied Physics A 123(11) (2017) 1–13.
26. S. Piñero, S. Camero, S. Blanco, Silver nanoparticles: Influence of the temperature synthesis on the particles' morphology, Journal of Physics: Conference Series, IOP Publishing, 2017, p. 012020.
27. J. Lu, J. Wang, K.T. Hassan, A. Talmantaite, Z. Xiao, M.R. Hunt, L. Šiller, Morphology control of nickel nanoparticles prepared in situ within silica aerogels produced by novel ambient pressure drying, Scientific reports 10(1) (2020) 1–9.
28. R. Maharsi, R. Septianto, F. Rohman, F. Iskandar, H. Devianto, Y. Budhi, Effect of temperature and precursor concentration on the morphology of Cu/γ-Al2O3 prepared via urea combustion method, Materials Research Express 4(4) (2017) 044002.
29. L. Yu, G. Zhang, Y. Wu, X. Bai, D. Guo, Cupric oxide nanoflowers synthesized with a simple solution route and their field emission, Journal of Crystal Growth 310(12) (2008) 3125–3130.
30. Z. Li, J. Wang, N. Wang, S. Yan, W. Liu, Y.Q. Fu, Z. Wang, Hydrothermal synthesis of hierarchically flower-like CuO nanostructures with porous nanosheets for excellent H2S sensing, Journal of Alloys and Compounds 725 (2017) 1136–1143.
31. H. Zhang, J. Feng, M. Zhang, Preparation of flower-like CuO by a simple chemical precipitation method and their application as electrode materials for capacitor, Materials Research Bulletin 43(12) (2008) 3221–3226.
32. Y. Zou, Y. Li, N. Zhang, X. Liu, Flower-like CuO synthesized by CTAB-assisted hydrothermal method, Bulletin of Materials Science 34(4) (2011) 967–971.

33. Z. Yang, J. Xu, W. Zhang, A. Liu, S. Tang, Controlled synthesis of CuO nanostructures by a simple solution route, Journal of Solid State Chemistry 180(4) (2007) 1390–1396.
34. L. Yu, G. Zhang, S. Li, Z. Xi, D. Guo, Fabrication of arrays of zinc oxide nanorods and nanotubes in aqueous solution under an external voltage, Journal of Crystal Growth 299(1) (2007) 184–188.
35. J. Liu, X. Huang, Y. Li, K. Sulieman, X. He, F. Sun, Hierarchical nanostructures of cupric oxide on a copper substrate: controllable morphology and wettability, Journal of Materials Chemistry 16(45) (2006) 4427–4434.
36. H. Chun Zeng, Ostwald ripening: a synthetic approach for hollow nanomaterials, Current Nanoscience 3(2) (2007) 177–181.
37. J. Wen, Y. Hu, K. Zhu, Y. Li, J. Song, High-temperature-mixing hydrothermal synthesis of ZnO nanocrystals with wide growth window, Current Applied Physics 14(3) (2014) 359–365.
38. J. Joo, B.Y. Chow, M. Prakash, E.S. Boyden, J.M. Jacobson, Face-selective electrostatic control of hydrothermal zinc oxide nanowire synthesis, Nature materials 10(8) (2011) 596–601.

Figures

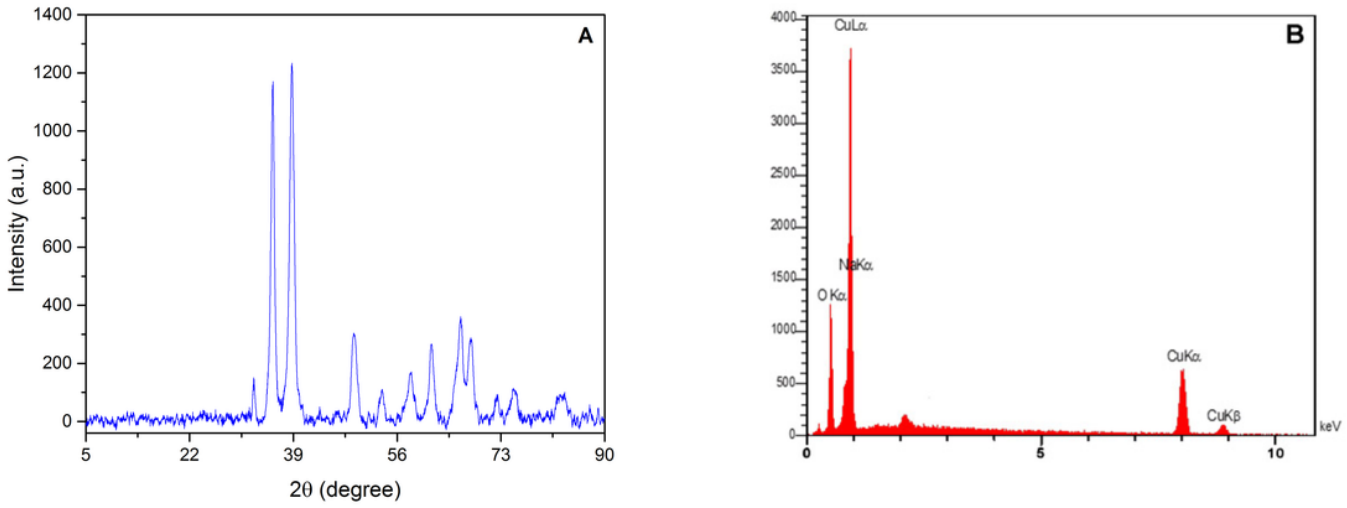


Figure 1

A) XRD pattern, and B) EDS analysis of synthesized CuO nanoparticles.

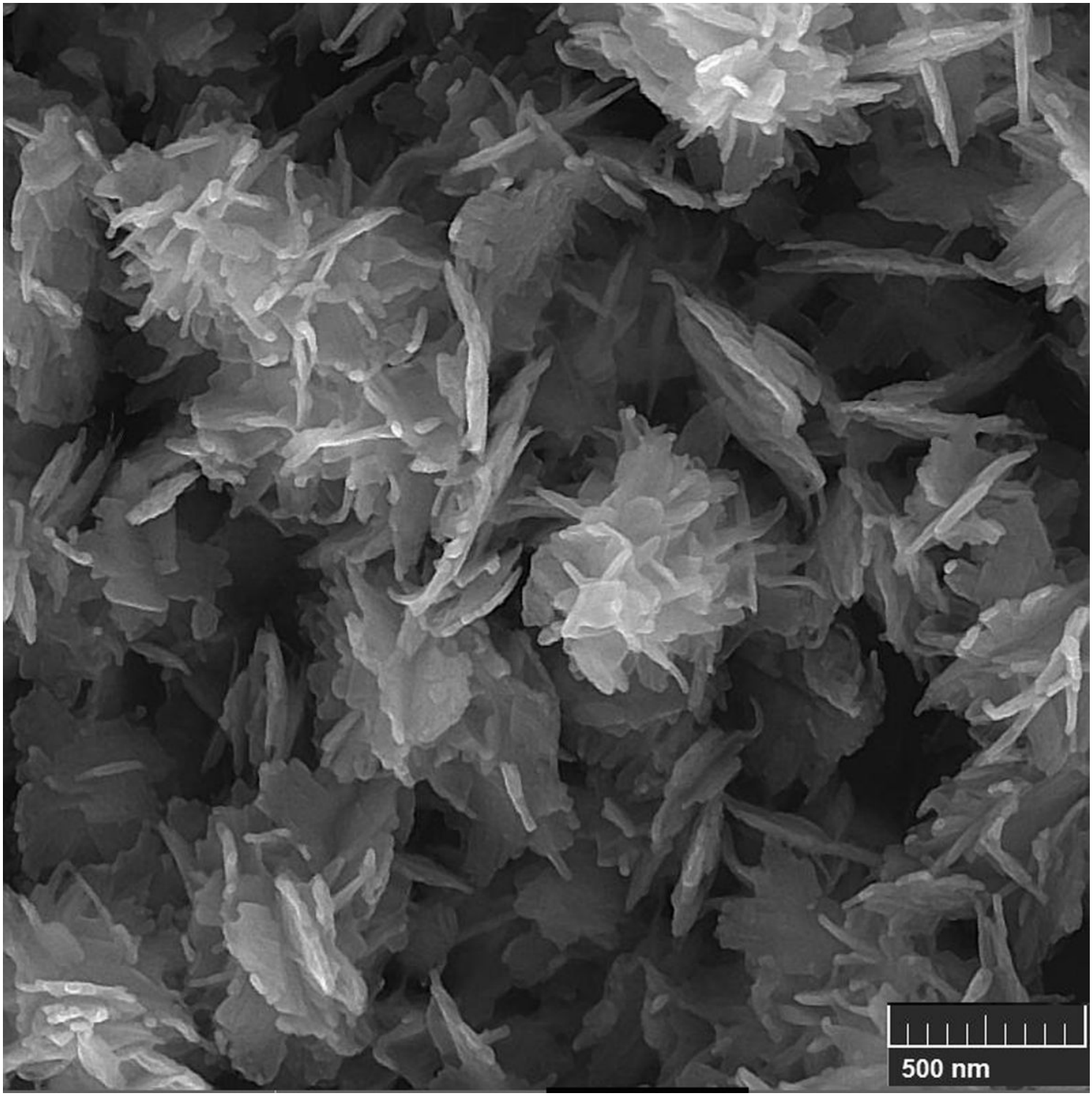


Figure 2

FESEM image of the synthesized CuO nanoparticles.

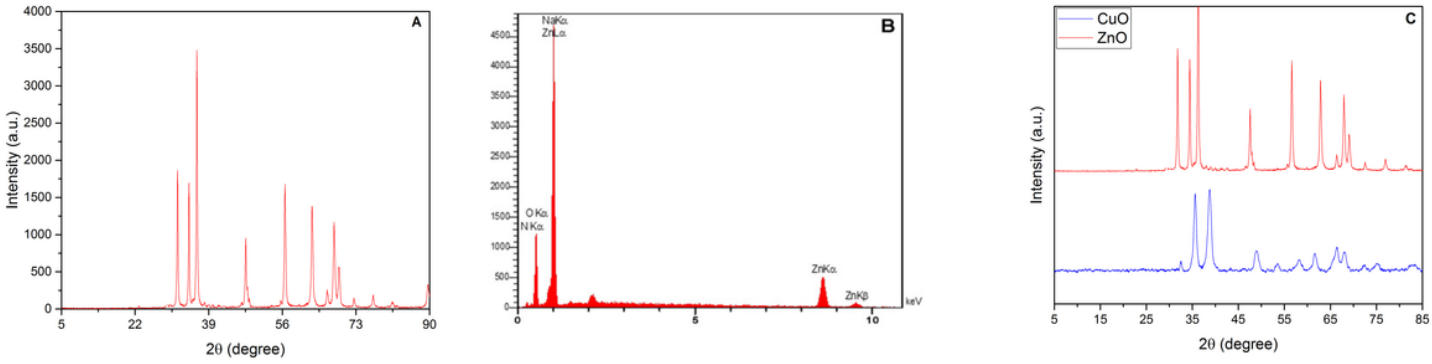


Figure 3

A) XRD pattern, B) EDS analysis of synthesized CuO nanoparticles, and C) normalized XRD patterns of synthesized CuO and ZnO nanoparticles.

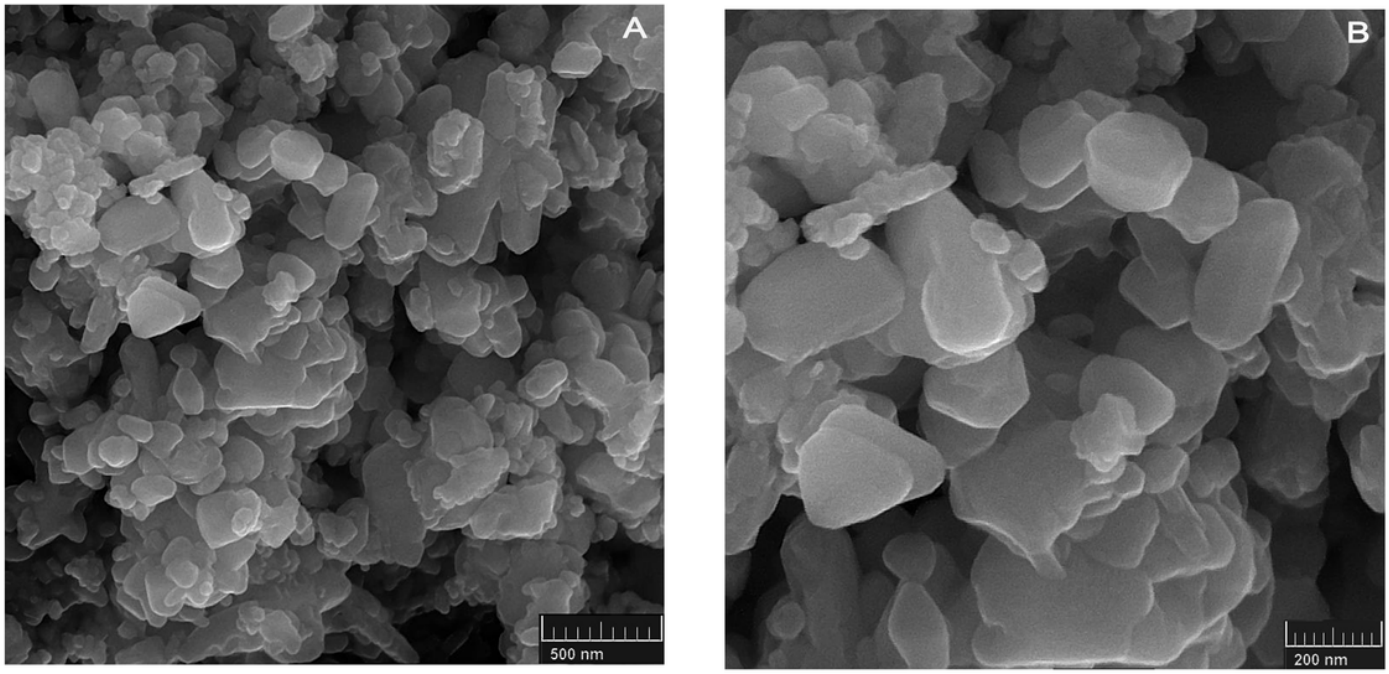


Figure 4

FESEM images of the synthesized ZnO nanoparticles with A) 75 kx, and B) 150 kx.